

## CHARACTERIZATION OF Er-DOPED GaAs DEPOSITED BY RESISTIVE EVAPORATION

M.C. Castro<sup>a,b</sup>; L.V.A. Scalvi<sup>a\*</sup>; L.O. Ruggiero<sup>a</sup>; E.A. Morais<sup>a</sup>

<sup>a</sup> UNESP, Dep. Física, C.P. 473, 17033-360 Bauru SP Brazil

<sup>b</sup> UNESP, Dep. Engenharia Elétrica, C.P. 473, 17033-360 Bauru SP Brazil

Received: July 30, 2003; Revised: October 18, 2004

Keywords: gallium arsenide, structural properties, erbium, resistive evaporation

### ABSTRACT

We have deposited Er-doped GaAs films by resistive evaporation technique, which is used by the first time with this purpose. The doping is incorporated into the matrix in the  $\text{ErCl}_3$  form. Results of X-ray spectroscopy of energy dispersion (EDX) show the Er incorporation into the film and results of X-ray diffraction (XRD) indicate single-crystal domains, randomly distributed throughout the structure. Sample transmittance in the near infrared is maximum in the 1500-1600nm range, coincident with the minimum absorption of optical fibers, and with the well known Er emission about 1540nm. Electrical characterization leads to striking results, since the resistance curve, in the dark, presents a peak about 65K.

### 1. INTRODUCTION

Rare-earth doping in III-V semiconductors is a promising field towards optoelectronic device production. Incorporation of rare-earth doping causes luminescence of host matrix due to a 4f core transition<sup>1</sup>.  $\text{Er}^{3+}$  presents several transitions<sup>2</sup>, being of particular interest the transition at 1.54 $\mu\text{m}$ , since it coincides with the minimum absorption of optical fibers based on silica. This transition is independent of nature of host matrix<sup>3</sup>, which affects only the fine structure of luminescence spectrum. The splitting of luminescence bands due to matrix nature suggests that various rare-earth centers are present<sup>4,5</sup>, probably due to interaction between excited rare-earth ions with matrix sites. Optical properties of various combinations of III-V semiconductors, doped with rare-earth ions have been widely investigated. However, electrical properties remains practically unknown<sup>6</sup>. R. A. Hogg et. Al.<sup>7</sup> report an optical anisotropy and preferential alignment of Er-2O center within the GaAs host along the growth direction which is responsible for the  $^4I_{13/2} \rightarrow ^4I_{15/2}$  intra-4f-shell luminescence. Recently X-ray diffraction and transmission electron microscopy have revealed GaAs nanoclusters randomly oriented in As-rich amorphous oxide outer shells<sup>8</sup>. Ion implantation has also been used to bury GaAs clusters inside silicon<sup>9</sup>. In this case GaAs exists in the form of nanocrystals which are oriented with respect to the silicon matrix. Films produced by depositing pre-formed mass-selected atomic clusters in the size range 1-10nm have obtained great deal of attention<sup>10</sup>. The possibilities of growth control allow great

flexibility in the creation of new types of nanostructure, which enables research on the fundamental behavior of matter of mesoscopic length scales. Besides, it has enormous potential in the creation of new material with large variety of properties. Semimetallic ErAs buried inside GaAs have been previously found<sup>11</sup>. In this case, spin disorder scattering produces a resistivity anomaly at low temperature, due to antiferromagnetic - paramagnetic phase boundary. Transport in ErAs:GaAs nanocomposites is also explained by hopping of bound magnetic polarons between nanoparticles of magnetic semimetallic ErAs<sup>12</sup> and a peak is obtained in the curve of resistivity versus applied magnetic field. Nanometer-sized magnetic particles in semiconductors are a potential means of memory storage and high-speed semiconductor electronics, while composites of magnetic and non-magnetic components are being developed for magnetic read heads<sup>13</sup>.

In this paper we present first results of GaAs produced with resistive evaporation technique and doped with  $\text{ErCl}_3$ . The resulting compound has the maximum infrared transmission in the 1500-1600 nm, coincident with the minimum absorption of optical fiber based on silica, and the Er is incorporated into the matrix as inferred from X-ray spectroscopy of energy dispersion (EDX). X-ray diffraction reveals the presence of crystalline regions into these films which can be associated with nanodomains of crystalline GaAs surrounded by amorphous phase of Ga-rich material. Films present a rather high resistivity due to compensation between  $\text{Er}^{3+}$  deep level and  $\text{Cl}^-$  donor level. The most striking result is a peak of resistance, observed around 65 K, in the dark, when this property is measured as function of temperature.

### 2. EXPERIMENTAL

Thin films of Er-doped GaAs were deposited on borosilicate substrates by resistive evaporation technique. Previous to deposition the doping compound ( $\text{ErCl}_3 \cdot 6\text{H}_2\text{O}$ ) is submitted to thermal annealing at 600°C, by 20 minutes, in order to eliminate the excess of water. This excess would make difficult to decrease the pressure inside the chamber. The deposition chamber is shown in figure 1, where the crucible is detailed in the inset. The distance between crucible and substrate is about 15 cm. Usually, the mass of doping is kept below 10% of total evaporating mass. The evaporation starts when pressure reaches about  $1 \times 10^{-5}$  Torr. Then, an electrical

\* scalvi@fc.unesp.br

current is passed through the Ta crucible. Current is increased until 4.8A, by 0.2A steps, lasting 5 minutes each until 1A and the same step lasting 10 minutes from 1A to 4.8A. The evaporation total time is about 3 hours. A plot of Ta crucible temperature as function of evaporation time is shown in figure 2. The crucible temperature was calibrated by using an optical pyrometer and the correspondence between Ta crucible temperature and current is shown in the inset of figure 2. For higher currents, the temperature is obtained by linear extrapolation of experimental data, which is clearly a straight line. This deposition technique has been used successfully for evaporation of other compounds and more details can be found elsewhere<sup>14,15</sup> ..

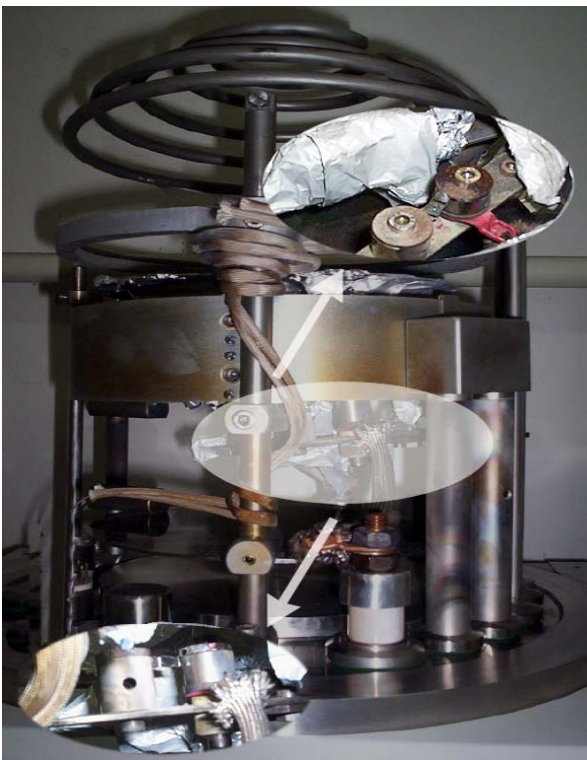


**Figure 1 – Evaporation chamber (without glass cover). Inset: Ta crucible disposition**

The series A of samples were produced to test whether was possible to introduce Er into GaAs matrix in the form of  $\text{ErCl}_3$ . Previously we had used  $\text{Er}_2\text{O}_3$ <sup>16</sup> and EDX results did not show Er in the composition. Then the amount of  $\text{ErCl}_3$  in total mass was exaggerated to 30% of total mass. As it will be seen in the next section, only one tenth of Er concentration introduced in the evaporating powder of series A was incorporated into the sample and besides, in order to introduce a fair amount of Er, to be considered a dopant, the series B of films were produced with only 9% in mass of  $\text{ErCl}_3$ . The evaporation procedure was exactly the same for both series of samples.

Films have been structurally characterized by electron scanning microscopy (ESM), X-ray spectroscopy of energy dispersion (EDX) and X-ray diffraction (XRD). ESM and EDX were carried out at CCDM-UFSCar, São Carlos, with a microscope Steroscan 440-LEO. XRD were carried out in a Rigaku diffractometer, coupled with a Cu source of 40kV

and 20 mA of current, and sampling with 10 degrees/minute and a fixed angle of 1 degree.

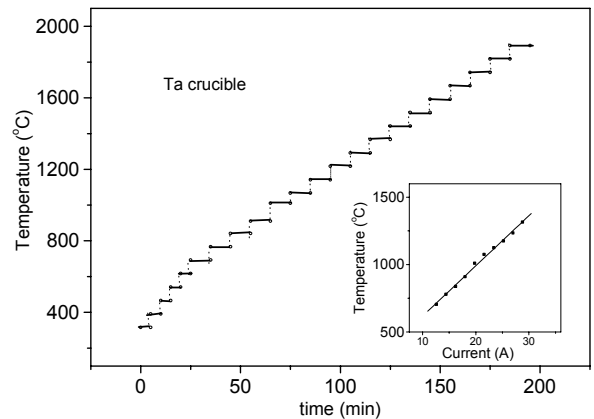


**Figure 2 – Ta crucible temperature x deposition time. Inset – Ta crucible temperature x current passing through the crucible, measured by an optical pyrometer**

Infrared transmittance was measured by a Nicolet spectrophotometer in the range  $400\text{--}7500\text{cm}^{-1}$ , with scanning rate of  $4\text{cm}^{-1}/\text{s}$ . To measure film resistance, electrical characterization measurements were done in the range 11-300K within a 0.1K of precision in an Cryogenics CCS-450 cryostat. The pressure in the chamber was kept below  $10^{-5}$ Torr. Resistance is measured with a Keithley electrometer. A diagram showing the experimental setup for electrical characterization is shown in figure 3.

### 3. RESULTS AND DISCUSSION

Figure 4 shows EDX results for sample A3. As it can be seen, only 3.5% of Er relative to total of relevant atoms in the matrix (Ga, As and Er) was detected. Smaller amount of Cl was also identified, which means that the chloride ions are not completely incorporated into the film, at least compared to the concentration of  $\text{Er}^{3+}$  ions. Si, Ca, Sn atoms, revealed by EDX, comes from the glass substrate. Au comes from the analysis system. The non-stoichiometric composition of 58% Ga to 39% of As is related to high volatility of As. Then a richer Ga deposition is expected. The Er concentration shall provide luminescence of GaAs matrix. This experiment must be carried out very soon. Another important point is that the thickness obtained from ESM results (not shown) is about  $2\ \mu\text{m}$ , which means that the deposition method is effective.

Figure 5 shows optical transmittance in the near infrared region for samples of A series. There is a broad band with a peak about  $6500\text{cm}^{-1}$ , which corresponds to about 1540nm. Although these samples show different transmission coefficient (sample A4 transmits only 35% where sample A3 transmits 56% at transmittance peak), the curve show the same shape. It means that this procedure is leading to reproductive films, which have Er incorporated into the matrix and present the highest transmittance coincident with the region of interest for communication via optical fibers based on silica. The bands observed between  $2500\text{--}3500\text{cm}^{-1}$

may be related to hydroxyl groups ( $\text{OH}^-$ )<sup>17</sup> which are not completely eliminated with the annealing at  $600^\circ\text{C}$  of the doping precursor ( $\text{ErCl}_3 \cdot 6\text{H}_2\text{O}$ ).

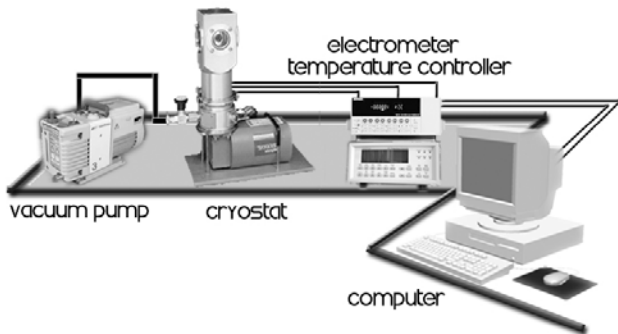


Figure 3 – Electrical characterization setup

MEM1: MET030924							
LiveTime =	100 s						
WINDOW LABEL	START keV	END keV	WIDTH CHANS	GROSS INTEGRAL	NET INTEGRAL	EFF. FACTOR	%AGE TOTAL
GaLa	1.04	1.14	6	23163	6747	1.00	57.83
AsLa	1.22	1.32	6	15566	4514	1.00	38.69
ErLa	6.86	7.02	9	1909	406	1.00	3.48

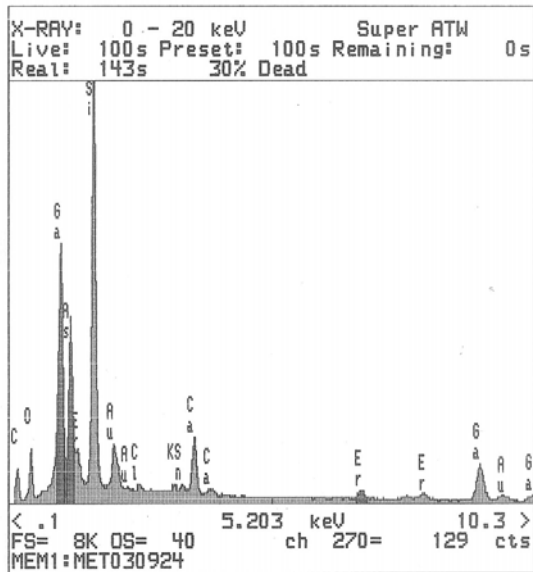


Figure 4- EDX measurements for films of series A

Figure 6 shows X-ray diffraction results for two samples of series B. As it can be seen, both samples present the same peaks, changing only the intensities, which are labeled in the figure. These peaks are located at  $27.3^\circ$ ,  $45.3^\circ$  and  $43.7^\circ$ , which are Bragg reflection planes from the (110), (220) and (311) planes, of GaAs single crystals. Dinh *et al.*<sup>8</sup> report exactly the same peaks for GaAs nanoclusters films grown on Si (100) wafer by a pulsed-laser deposition. The XRD pattern shown in figure 6 raises the possibility of cluster formation also in our films. XRD carried out on films of series A does not show any peak, instead it shows the broad band characteristic of amorphous films. These results

reinforce the possibility of cluster formation, since resistive evaporation technique leads essentially to amorphous films. The observed peaks in Er-doped GaAs deposited films may be originated from crystalline clusters randomly oriented and distributed throughout the film. In this case, the matrix is composed of an Ga-rich material, in agreement with the EDX- results, shown in figure 4. The Er-doping atoms position into the matrix is still unknown.

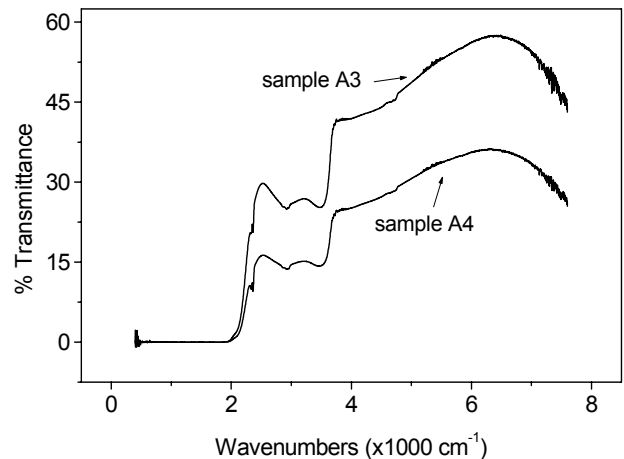


Figure 5 – Near infrared transmittance for GaAs films of series A

Figure 7 corresponds to resistance x temperature measurements for films of GaAs doped with  $\text{ErCl}_3$ . Although the curves shown in figure 7 and in the inset present rather different resistance, the curve shape is essentially preserved. The uneven behavior of the curve of the inset is due to the high resistance value, where equipment limitations become important. The existing peak of these curves is rather unexpected and although a slight shift is observed, this peak is present in all the films deposited with  $\text{ErCl}_3$  doping. The position of this peak shifts a little from sample to sample, but it is always located between 55 and 70 K. The doping with Cl may lead to a high donor concentration. The strong ionicity of this atom has led to effective n-type doping in semiconductors. Studies in the semiconductor ZnSe for instance, show that  $\text{Cl}^-$  ion is a very efficient donor, presenting activation energies in the range 25-31meV<sup>18</sup>. By other hand,  $\text{Er}^{3+}$  ion creates an electron trap in GaAs at 0.67eV from the conduction band<sup>6</sup>. Therefore the simultaneous presence of these two doping elements in the matrix justifies the high resistivity obtained from these films, since there is a high degree of charge compensation. For instance, the room temperature resistivity of the sample of figure 7 is about 400 ohm.cm.

The peak observed in the resistance x temperature curve is a striking result. Previously we had observed this behavior only in GaAs based alloys when illuminated with monochromatic light<sup>19</sup>. Considering that the measurement of figure 7 is carried out in the dark, there is no photoinduced effect in this sample. The actual explanation of this temperature effect is the subject of our present

investigation. At this point it must be mentioned that an antiferromagnetic-paramagnetic phase transition has been reported for ErAs epitaxial layers buried in GaAs for much lower temperature<sup>11</sup> and a similar effect for nanocomposites of ErAs:GaAs<sup>12</sup>. Both effects are related to the existence of a positive magnetoresistance for lower applied magnetic field. Then, an experiment including magnetic field may bring light to the results presented in figure 7. The magnetic properties of these films shall be a matter of our next research. We have observed that films produced with excess of Er (series A) attract small pieces of iron and then, it suggests that these films may present magnetic particles and be very suitable to investigation of transport.

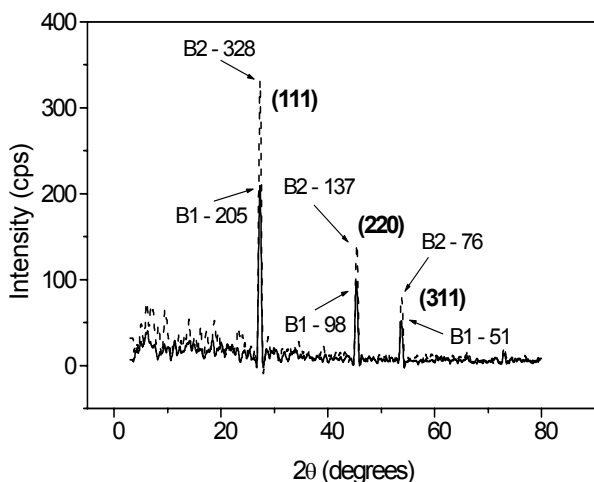


Figure 6 – X-ray diffraction for GaAs films of series B

#### 4. CONCLUSION

We have produced a Er-doped GaAs using a new technique and new precursors. Results presented here are the first observations on the characterization of these materials. These results indicate a brand new series of properties which deserves a deep investigation. Besides the high transmittance in the infrared region, these films presents X-ray peaks which may be related to crystalline domains into the matrix. A striking peak in the curve of resistance x temperature, in the dark, is observed for all the films of GaAs doped with ErCl<sub>3</sub>. Although the interesting and well known 4f transition of Er in the matrix has not been obtained yet, these films present magnetic properties, which may be related to the presence of clusters. The nanoscopic or microscopic nature of these crystallites is a matter for future research, based mainly on their electrical and magnetic properties.

#### ACKNOWLEDGEMENTS

The authors would like to thank Prof. Margarida J. Saeki for the IR-transmittance measurements and Prof. Maximo Siu Li for the start of this research. The authors also thank

Brazilian financial sources: CAPES, CNPq, FAPESP and MCT-PRONEX.

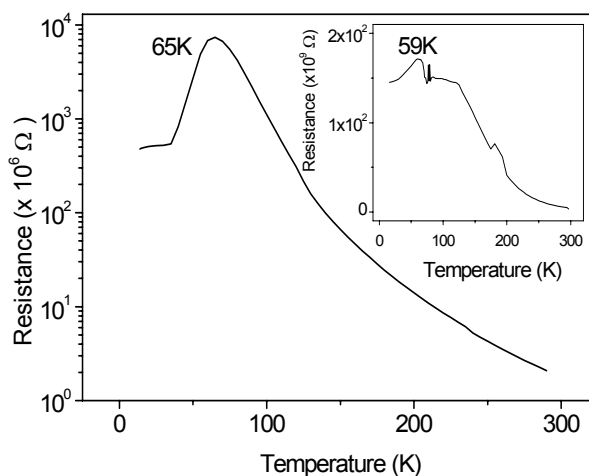


Figure 7 – Resistance x temperature in the dark for GaAs:ErCl<sub>3</sub> for series A samples

#### REFERENCES

1. TAKARABE, K., *Phys. Stat. Sol. (b)* 198 (1996) 211.
2. MORAIS, E.A.; RIBEIRO, S.J.L.; SCALVI, L.V.A.; SANTILLI, C.V.; RUGGIERO, L.O.; PULCINELLI, S.H.; MESSADDEQ, Y., *J. Alloys and Comp.* 344 (2002) 217.
3. COFFA, S.; FRANZO, G.; PRIOLO, F.; POLMAN, A.; SERNA, R., *Phys. Rev. B* 49 (1994) 16313.
4. TAKAHEI, K.; TAGUCHI, A.; HOGG, R.A., *J. Appl. Phys.* 82 (1997) 3997.
5. HOGG, R.A.; TAKAHEI, K.; TAGUCHI, A., *Phys. Rev. B* 56 (1997) 10255.
6. SEGHIER, D.; BENYATTOU, T.; KALBOUSSI, A.; MONEGER, S.; MARRAKCHI, G.; GUILLOT, G.; LAMBERT, B.; GUIVARC'H, A., *J. Appl. Phys.* 75 (1994) 4171.
7. HOGG, R.A.; TAKAHEI, K.; TAGUCHI, A.; HORIKOSHI, Y., *Appl. Phys. Lett.*, 68 (1996) 3317.
8. DINH, L.N.; HAYES, S.; SAW, C.K.; MCLEAN, W.; BALOOCH, M.; REAMER, J.A., *Appl. Phys. Lett.*, 75 (1999) 2208.
9. WHITE, C.W.; BUDDAI, J.D.; ZHU, J.G.; WITHROW, S.P.; AZIZ, M.J. *Appl. Phys. Lett.* 68 (1996) 2389.
10. BINNS, C., *Surf. Sci. Reports* 44 (2001) 1.
11. ALLEN, S.J.; TABATABAIE, N.; PALMSTROM, C.J.; HULL, G.W.; SANDS, T.; DE ROSA, F.; GILCHRIST, H.L.; GARRISON, K.C., *Phys. Rev. Lett.* 62 (1989) 2309.
12. SCHMIDT, D.R.; PETUKHOV, A.G.; FOYGEL, M.; IBBERTSON, J.P.; ALLEN, S.J., *Phys. Rev. Lett.* 82 (1999) 823.
13. SCHMIDT, D.R.; IBBERTSON, J.P.; BREHMER, D.E.; PALMSTROM, C.J.; ALLEN, S.J., *Giant Magnetoresistance of Self-assembled ErAs Islands in GaAs*, MRS Symp. Proc. v. 475, p. 251, 1997.
14. OLIVEIRA, L.; SIU LI, M., *Thin Solid Films* 268 (1995) 30.
15. OLIVEIRA, L.; CRUZ, C.M.G.S.; SILVA, M.A.P.; SIU LI, M., *Thin Solid Films* 250 (1995) 273.
16. CASTRO, M.C.; SCALVI, L.V.A.; TEODORO, M.M.; MORAIS, E.A.; RUGGIERO, L.O., *Influência da*

- temperatura no precursor e Evidências da Incorporação do terra-rara na deposição de GaAs:Er* (portuguese), Anais da 1a. Conferência Brasileira sobre Temas de Tratamentos Térmicos, p. 171, 2003 (pub. CR-ROM)
17. LIN, Y.J.; WU, C.S., *Surf. & Coat. Technol.* 88 (1996) 239.
  18. MELO, O.; HERNANDEZ, L.; MELENDEZ-LIRA, M.; RIVIERA-ALVAREZ, Z.; HERNANDEZ-CALDERON, I., SBMO/IEEE MTT-5 *Microwave and Optoelectronics Conference'95 Proc.*, p. 455, 1995
  19. TAQUECITA, M.H.; SCALVI, L.V.A.; OLIVEIRA, L.; SIU LI, M.; PARREIRA, S.B., *Rad. Eff. & Def. Solids* 146 (1998) 175.